Double Exchange and Vibronic Coupling in Mixed Valence Systems. Origin of the Broken-Symmetry Ground State of $[Fe_3S_4]^0$ Cores in Proteins and Models†

Sergueï A. Borshch,*,‡ Emile L. Bominaar, Geneviève Blondin, and Jean-Jacques Girerd*

Contribution from the Laboratoire de Chimie Inorganique, URA CNRS 420, Institut de Chimie Moléculaire d'Orsay, Université Paris-Sud, 91405 Orsay, France

Received October 16, 1992

Abstract: The origin of the pair-delocalized ground state of spin $S = 2$, observed in chemically symmetric mixed-valence $[Fe_3S_4]^0$ cores present in proteins and synthetic models, is analyzed in the framework of an effective-Hamiltonian model, comprising terms for excess-electron transfer (leading to double-exchange coupling of the paramagnetic Fe(III) cores), vibronic coupling (trapping the excess electron), and antiferromagnetic exchange. The basic mechanisms underlying the inhomogeneous electron distributions in trinuclear mixed-valence clusters with paramagnetic ion cores are illustrated in a simple model with electronic structure d^1-d^1-d^2. The adiabatic potential surfaces of the system are determined and their extremal points, corresponding to definite electron distributions, are ascertained. The electron distributions depend essentially on the ratio of transfer parameter and vibronic trapping energy: $\beta/(\lambda^2/2\kappa)$. For small ratios, the excess electron is site-trapped; for larger values (≥ 1) the delocalization behavior depends on the nature of the electronic state considered. In case of a degenerate manifold including different irreducible representations (A + E in C_{3v} symmetry), the excess electron is trapped in a pair-delocalized state, in which the electronic charge is accumulated at two sites of the trinuclear system. Analysis of the triiron unit (represented by electronic structure d^5-d^5-d^6) reveals, for $\beta > 0$, a highly degenerate electronic ground state, including spin levels ranging from $S = 0$–6. The ground manifolds for $S = 1, \ldots, 4$ are, for $\beta > 0$, 'A + E'-degenerate and give rise to broken-symmetry, pair-delocalized ground states. The excess electron in these states is not strictly confined to a pair of sites; there is a finite probability density of finding the electron at the remaining center. The smallest density (and strongest vibronic stabilization) is found for spin $S = 2$: the conjunction of electron-transfer interaction and vibronic coupling leads to a pair-delocalized ground state of spin $S = 2$ for $\beta/(\lambda^2/2\kappa) \geq 1$. The condition is satisfied by estimates of the ratio in trinuclear iron–sulfur clusters, which explains the ground state observed therein. The calculated magnetic hyperfine parameters are in good agreement with experiment. Introduction of antiferromagnetic exchange does not change the main conclusions obtained without this interaction.

Introduction

Iron–sulfur proteins are implied in different biochemical processes, thereby acting as electron-transfer agents or as catalytic systems like in aconitase and nitrogenase.[1-5] The biological importance of the systems has stimulated synthetic efforts to modelize the active sites.[6] The natural systems as well as the models have been subjected to intensive structural and spectroscopic studies.[7-9]

The functions of many of these systems derive from the ability of the central iron–sulfur unit to store different numbers of electrons. The ensuing mixed-valence oxidation levels represent a set of Fe(III) cores accommodating one or several "excess" electrons.

In proteins with dinuclear clusters the excess electron is found, by Mössbauer spectroscopy, to be mainly localized at one iron site.[10] The observation of the same phenomenon in chemically symmetric model compounds led Holm et al. to the conclusion that the localization of the excess electron is not caused by the protein surrounding but is an intrinsic property of $[Fe_2S_2]^+$ clusters.[11]

In natural trinuclear $[Fe_3S_4]^0$ and tetranuclear "cubane" $[Fe_4S_4]^{3+}$ clusters with formal oxidation states 2Fe(III) + Fe(II) and 3Fe(III) + Fe(II), respectively, the delocalization of the excess electron is also restricted but now to a pair of sites. An example of pair localization is found in the reduced form of the trinuclear iron–sulfur cluster in ferredoxin II (FdII) from *Desulfovibrio gigas*.[12] Meanwhile a structure fairly close to trigonal symmetry is found by X-ray crystallography in the oxidized state of the cluster.[13,14] Recently, the same electron localization pattern was observed in triiron subunits of synthetic clusters with MFe_3S_4 (M = Mo, W, Fe) cores with equivalent iron sites.[15,16] As was pointed out in ref 15 this inhomogeneous electron distribution must be also an intrinsic property of the $[Fe_3S_4]^0$ clusters.

† Dedicated to Prof. R. H. Holm on the occasion of his 60th birthday.

‡ On leave from Institute of Chemistry, Academy of Sciences of Moldova, Kishinev. Present address: Institut de Recherche sur la Catalyse, CNRS, 69626 Villeurbanne, France.

(1) Beinert, H.; Kennedy, M. C. *Eur. J. Biochem.* **1990**, *186*, 5–15.
(2) Lindahl, P. A.; Kovacs, J. A. *Clusters* **1990**, *1*, 29–73.
(3) Eady, R. R. *Advances in Inorganic Chemistry*; Sykes, A. G., Ed.; Academic Press: New York, 1991; Vol. 36, pp 77–102.
(4) Burgess, B. *Chem. Rev.* **1990**, *90*, 1377–1406.
(5) *Advances in Inorganic Chemistry*; Sykes, A. G., Ed.; Academic Press: New York, 1992; Vol. 38.
(6) Holm, R. H.; Ciurli, S.; Weigel, J. A. *Progr. Inorg. Chem.* **1990**, *38*, 1–74.
(7) Trautwein, A. X.; Bill, E.; Bominaar, E. L.; Winkler, H. *Structure and Bonding*; Springer: Berlin, Heidelberg, 1991; Vol. 78, pp 1–95.
(8) Banci, L.; Bertini, I.; Briganti, F.; Luchinat, C. *New J. Chem.* **1991**, *15*, 467–477.
(9) Bertrand, P.; Guigliarelli, B.; More, C. *New J. Chem.* **1991**, *15*, 445–454.
(10) Cammack, R.; Dickson, D. P. E.; Johnson, C. E. *Iron–Sulfur Proteins*; Lovenberg, W., Ed.; Academic Press: New York, 1977; Vol. III, pp 283–330.
(11) Mascharak, P. K.; Papaefthymiou, G. C.; Frankel, R. B.; Holm, R. H. *J. Am. Chem. Soc.* **1981**, *103*, 6110–6116.
(12) Papaefthymiou, V.; Girerd, J.-J.; Moura, I.; Moura, J. J. G.; Münck, E. *J. Am. Chem. Soc.* **1987**, *109*, 4703–4710.
(13) Kissinger, C. R.; Adman, E. T.; Sieker, L. C.; Jensen, L. H. *J. Am. Chem. Soc.* **1988**, *110*, 8721–8723.
(14) Kissinger, C. R.; Sieker, L. C.; Adman, E. T.; Jensen, L. H. *J. Mol. Biol.* **1991**, *219*, 693–715.
(15) Weigel, J. A.; Srivastava, K. K. P.; Day, E. P.; Holm, R. H. *J. Am. Chem. Soc.* **1990**, *112*, 8015–8023.
(16) Coucouvanis, D.; Al-Ahmad, S. A.; Salifoglou, A.; Papaefthymiou, V.; Kostikas, A.; Simopoulos, A. *J. Am. Chem. Soc.* **1992**, *114*, 2472–2482.

0002-7863/93/1515-5155$04.00/0

The investigations of the trinuclear iron–sulfur clusters reveal furthermore that the spin structures in their ground states are similar.[12,15,16] The iron ions are in high-spin states: $S_{Fe(II)} = 2$ and $S_{Fe(III)} = {}^5/_2$. The Mössbauer spectra can be interpreted in terms of a model with the spin of the delocalized pair, $S_{ij} = {}^9/_2$, coupled to the spin of the remaining Fe(III) ion to give the total cluster spin $S = 2$. The stabilization of a high-spin state in the dinuclear subunit is probably a consequence of double-exchange coupling between the iron core spins, caused by the delocalization of the excess electron.[17–22] The origin of the partial delocalization in the iron–sulfur clusters remains, however, obscure in purely electronic treatments of these systems and is the subject of this paper.

The concept of vibronic interaction is of primary importance for the description of electron localization in mixed-valence systems.[23,24] Localization of the excess electron in symmetric mixed-valence systems is always accompanied by a symmetry breaking of the nuclear framework, which manifests the vibronic (nonadiabatic) mixing of electronic states obtained in the symmetric nuclear configuration. Theoretical analysis of magnetic mixed-valence dinuclear systems shows that the combination of double exchange and vibronic coupling gives rise to spin-dependent electron delocalization patterns.[17] Recently, it was shown[25] that the two interactions can lead to delocalization over a pair in the spin-quintet state of a symmetric $[Fe_3S_4]^0$ cluster.

Although a number of significant features of the $[Fe_3S_4]^0$ clusters have been elucidated, there remain a number of important questions to be answered: what is the origin of the $S = 2$ ground state with the excess electron delocalization over a pair, and how is one to interpret the spin composition of this state? Is delocalization in a pair only present in the spin $S = 2$ state of the iron cluster, or are we dealing with a more general phenomenon?

The paper is organized as follows. The electronic dinuclear states formed by double exchange are introduced in a symmetry-adapted way, suitable for further discussion of the trinuclear system. The basic mechanism behind the partial electron localization in trinuclear clusters due to the common action of double exchange and vibronic coupling is illustrated in the simplest mixed-valence cluster adapted to such a study: the d^1-d^1-d^2 case with one excess electron and paramagnetic core spins $S_i^0 = 1/2$. The spin composition of the eigenstates is analyzed. Subsequently, we extend our model to the case of electronic configuration, d^5-d^5-d^6, characteristic for $[Fe_3S_4]^0$ clusters. It is shown that the spin $S = 2$ state with electron delocalization over a pair becomes the ground state by double exchange and vibronic interaction. The magnetic hyperfine parameters of FdII are analyzed within the model. The model parameters relevant to the actual systems are estimated, and the influence of antiferromagnetic exchange on spin-state energies is discussed.

Double Exchange in Dinuclear Clusters: A Molecular Orbital Approach

The concept of double-exchange coupling was introduced by Zener for the explanation of the ferromagnetism in a number of mixed-valent semiconductors[19,20] and was further developed by several groups in studies of mixed-valence clusters.[17,18,26–28] The mechanism is based on the application of Hund's rule in the description of arrays of paramagnetic ions in the presence of delocalized excess electrons. The coupling mechanism is illustrated in the following diagram, displaying a mixed-valence dimer

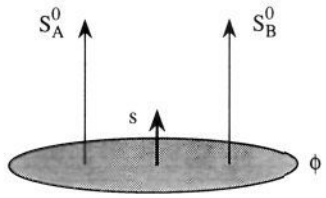

(1)

containing two paramagnetic ion cores with spins S_A^0 and S_B^0, and one itinerant ("excess") electron of spin s. The excess electron, occupying molecular orbital ϕ, penetrates the paramagnetic cores of the two ions. The resulting spatial overlaps lead to exchange interactions between the excess electron and the electrons of the two paramagnetic ion cores. These interactions align the ion core spins with respect to the excess-electron spin and give rise to an effective ferromagnetic coupling of the ion core spins.

A theoretical analysis of the double-exchange coupling in symmetric dimers has been given in a study by Anderson and Hasegawa.[20] Therein analytical expressions of the complete spectrum of spinstate energies and eigenstates are derived, starting from a localized description of the excess electron. In the next section we briefly summarize the theory of Anderson and Hasegawa. Subsequently, the electronic eigenstates will be expressed in terms of molecular orbitals, in order to facilitate afterwards the analysis of the trinuclear systems. As there exist some formal differences in the descriptions of systems d^n-d^{n+1} with less than half-filled shells ($n < 5$) and with half or more than half-filled shells ($n \geq 5$), we shall treat the two cases separately.

Less than Half-Filled d Shells. Anderson and Hasegawa consider a symmetric dinuclear mixed-valence system, AB, containing an excess electron which is assumed to occupy the orthogonal orbitals a and b, localized at the centers A and B, respectively. The electronic states corresponding to occupation of orbitals a and b do not diagonalize the operators for the kinetic energy and the effective field in which the electron moves. The nondiagonal interaction is expressed by transfer integral β. Under the above assumptions, the electronic Hamiltonian is reduced to an effective operator of the form

$$H_t = \beta t_{AB} \tag{1}$$

in which the operator t_{AB} is defined by its action on the functions $|a\rangle$ and $|b\rangle$: $t_{AB}|a\rangle = |b\rangle$ and $t_{AB}|b\rangle = |a\rangle$. In case of diamagnetic ion cores, diagonalization of eq 1 yields the molecular orbitals

$$\phi_\pm = \frac{1}{\sqrt{2}}(a \pm b) \tag{2}$$

and energy eigenvalues $E = \pm\beta$, where the signs correspond to those in eq 2.

The electronic states and energies of a binuclear mixed-valence system with paramagnetic ion cores, $S_A^0 = S_B^0 = S^0 \neq 0$, depend on the total spin S_{AB} of the dimer. A set of basis functions for the dimer is given by

$$|(S_A^0,s)S_A,S_B^0,S_{AB};a\rangle \tag{3a}$$

(17) Girerd, J.-J. *J. Chem. Phys.* **1983**, *79*, 1766–1775.
(18) Noodleman, L.; Baerends, E. J. *J. Am. Chem. Soc.* **1984**, *106*, 2316–2327.
(19) Zener, C. *Phys. Rev.* **1951**, *82*, 403–405.
(20) Anderson, P. W.; Hasegawa, H. *Phys. Rev.* **1955**, *100*, 675–681.
(21) Blondin, G.; Girerd, J.-J. *Chem. Rev.* **1990**, *90*, 1359–1376.
(22) Blondin, G.; Borshch, S. A.; Girerd, J.-J. *Comments Inorg. Chem.* **1992**, *12*, 315–340.
(23) Piepho, S. B.; Krausz, E. R.; Schatz, P. N. *J. Am. Chem. Soc.* **1978**, *100*, 2996–3005.
(24) Bersuker, I. B.; Borshch, S. A. In *Advances in Chemical Physics*; Prigogine, I., Rice, S. A., Eds.; John Wiley: New York, 1992; Vol. 81, pp 703–782.
(25) Borshch, S. A.; Chibotaru, L. F. *Chem. Phys.* **1989**, *135*, 375–380.
(26) Borshch, S. A.; Kotov, I. N.; Bersuker, I. B. *Sov. J. Chem. Phys.* **1985**, *3*, 1009–1016.
(27) Belinskii, M. I.; Tsukerblat, B. S.; Gerbeleu, N. V. *Sov. Phys. Solid State* **1983**, *25*, 497–498.
(28) Borshch, S. A.; Kotov, I. N.; Bersuker, I. B. *Chem. Phys. Lett.* **1984**, *111*, 264–270.

$$|S^0_A,(s,S^0_B)S_B,S_{AB};b\rangle \quad (3b)$$

which are depicted by diagrams (2) and (3), respectively. The excess electron in functions eqs 3a and 3b occupy the orbitals a and b. As we are dealing with a less than half-filled d shell, the excess-electron spin is coupled parallel to the core spin, e.g., $(S^0_A, s)\ S_A = S^0 + {}^1/_2$ in expression eq 3a, according to Hund's rule. Subsequently, the spin S_A and the spin of the opposite site, S^0_B, are coupled to resultant total spin S_{AB}. The total spin S_{AB}

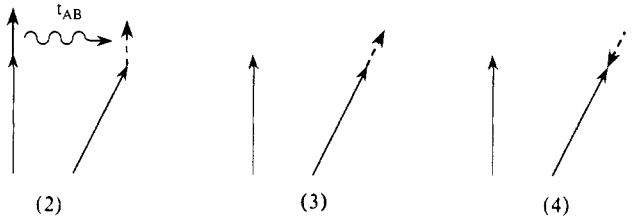

can be depicted by the vector sum of the core- and excess-electron spins, and the value of S_{AB} depends on the angle between the core spins: states of maximum spin, $S_{AB} = S^0_A + S^0_B + {}^1/_2$, correspond to a parallel alignment of the core spins (diagram (1)) and states of lower spin to tilted configurations, such as the one shown in the diagram (2).

The action of the transfer operator eq 1 on basis state eq 3a transfers the excess electron (diagram (1)) from orbital a to b; its spin, however, remains coupled parallel to core spin S^0_A, leading to the dimer state $|(S^0_A, s)\ S_A = S^0 + {}^1/_2, S^0_B, S_{AB};b\rangle$ (see also diagram (2)). The state can be expressed as a linear combination of the Hund's rule respecting basis state eq 3b (diagram (3)) and a state which violates this rule (diagram (4)). We shall assume that the latter state is separated by a large energy gap from the ground state, so that it may be ignored. Formally, this restriction is achieved (see ref 21) by introducing the projection operator P_0 onto the space of Hund's rule respecting states in the expression for the transfer operator

$$H_t = \beta P_0 t_{AB} P_0 \quad (4)$$

The matrix element of the electron transfer is reduced by the coefficient of state eq 3b in the linear combination. The coefficient is related to the projection factor of the spin function of the transferred electron (quantized along spin S^0_A) onto the spin function which is quantized along spin S^0_B. The expression for the projection factor $\langle (S^0_A, s)S_A = S^0 + {}^1/_2, S^0_B, S_{AB}|S^0_A, (s, S^0_B)\ S_B = S^0 + {}^1/_2, S_{AB}\rangle$ is readily evaluated by using the formula for spin-recoupling coefficients given by Racah (see, e.g., ref 29), and reads $(S_{AB} + {}^1/_2)/(2S^0 + 1)$. Hence, application of operator eq 4 on the basis function eq 3a gives

$$H_t|(S^0_A, s)S_A = S^0 + {}^1/_2, S^0_B, S_{AB};a\rangle = \beta\frac{S_{AB} + {}^1/_2}{2S^0 + 1}|S^0_A, (s, S^0_B)S_B = S^0 + {}^1/_2, S_{AB};b\rangle \quad (5)$$

Diagonalization of the effective Hamiltonian eq 4 yields the energy spectrum

$$E^{S_{AB}}_{\pm} = \pm\beta\frac{S_{AB} + {}^1/_2}{2S^0 + 1} \quad (6)$$

and the eigenfunctions

$$\Phi^{S_{AB}}_{\pm} = \frac{1}{\sqrt{2}}[|(S^0_A, s)S_A = S^0 + {}^1/_2, S^0_B, S_{AB};a\rangle \pm |S^0_A,(s, S^0_B)S_B = S^0 + {}^1/_2, S_{AB};b\rangle] \quad (7)$$

where the subscripts $\pm$ correspond to the signs in eq 6.

We will now pass in eq 7 from the localized orbitals, a and b, to the molecular orbitals given in eq 2. To that end, we adopt another coupling scheme in which the core spins S^0_A and S^0_B are coupled first to resultant spin S^0_{AB}, which is then coupled to the spin, s, of the itinerant electron. Using again the method for spin recoupling given by Racah, one obtains the following expressions for the eigenfunctions:

$$\Phi^{S_{AB}}_{\pm} = -\left[\frac{2S^0 - S_{AB} + {}^1/_2}{4(2S^0 + 1)}\right]^{1/2}[|(S^0_A, S^0_B)S^0_{AB} = S_{AB} + {}^1/_2, s, S_{AB};a\rangle \mp |(S^0_A, S^0_B)S^0_{AB} = S_{AB} + {}^1/_2, s, S_{AB};b\rangle] + \left[\frac{2S^0 + S_{AB} + {}^3/_2}{4(2S^0 + 1)}\right]^{1/2}[|(S^0_A, S^0_B)S^0_{AB} = S_{AB} - {}^1/_2, s, S_{AB};a\rangle \pm |(S^0_A, S^0_B)S^0_{AB} = S_{AB} - {}^1/_2, s, S_{AB};b\rangle] \quad (8)$$

The multielectronic wavefunctions are constructed from antisymmetrized products of spin orbitals. As the antisymmetrization operator is linear with respect to the one-electron states, we can combine the first and second term in eq 8 as well as the third and fourth term into single configurations, which leads to the expression

$$\Phi^{S_{AB}}_{\pm} = -\left[\frac{2S^0 - S_{AB} + {}^1/_2}{2(2S^0 + 1)}\right]^{1/2}|(S^0_A, S^0_B)S^0_{AB} = S_{AB} + {}^1/_2, s, S_{AB};\phi_{\mp}\rangle + \left[\frac{2S^0 + S_{AB} + {}^3/_2}{2(2S^0 + 1)}\right]^{1/2}|(S^0_A, S^0_B)S^0_{AB} = S_{AB} - {}^1/_2, s, S_{AB};\phi_{\pm}\rangle \quad (9)$$

It is seen that the electronic eigenstates are linear combinations of two configurations in which the excess electron occupies the molecular orbitals ϕ_+ and ϕ_-. For maximum spin, $S_{AB} = 2S^0 + {}^1/_2$, the coefficient of the first term in eq 9 is zero. The eigenstates $\Phi^{S_{AB}}_+$ and $\Phi^{S_{AB}}_-$ are then equal to single configurations in which the excess electron occupies the orbitals ϕ_+ and ϕ_-, respectively. For lower values of the spin S_{AB}, the ratios of the coefficients of linear combination in the eigenfunctions eq 9 approach one. These features are demonstrated in Table I in the example of the dimer d^1-d^2.

Table I. Energies and Wavefunctions for the d^1-d^2 Double-Exchange Problem

energy	wavefunction
$+\beta$	$\Phi^{3/2}_+ = \|S^0_{AB} = 1, S_{AB} = \frac{3}{2}; \phi_+\rangle$
$+\frac{1}{2}\beta$	$\Phi^{1/2}_+ = \frac{\sqrt{3}}{2}\|S^0_{AB} = 0, S_{AB} = \frac{1}{2}; \phi_+\rangle - \frac{1}{2}\|S^0_{AB} = 1, S_{AB} = \frac{1}{2}; \phi_-\rangle$
$-\frac{1}{2}\beta$	$\Phi^{1/2}_- = \frac{\sqrt{3}}{2}\|S^0_{AB} = 0, S_{AB} = \frac{1}{2}; \phi_-\rangle - \frac{1}{2}\|S^0_{AB} = 1, S_{AB} = \frac{1}{2}; \phi_+\rangle$
$-\beta$	$\Phi^{3/2}_- = \|S^0_{AB} = 1, S_{AB} = \frac{3}{2}; \phi_-\rangle$

The symmetries of the eigenstates can be easily deduced from expressions eq 9, once the symmetry group of the dinuclear system and the orbitals a and b are known. For instance, in C_s symmetry, when the orbitals a and b of the dinuclear system are interchanged by reflection with respect to a perpendicular mirror plane bisecting the axis AB, the states $\Phi^{3/2}_+$ and $\Phi^{1/2}_-$ transform according to the representation A″ and the states $\Phi^{1/2}_+$ and $\Phi^{3/2}_-$ according to the representation A′.

Half or More Than Half-Filled d Shells. The excess electron in dinuclear transition–ion complexes of electronic structure d^n-d^{n+1} with $n \geq 5$, e.g., the Fe(III)Fe(II) system, is necessarily occupying a d orbital which is already half-occupied by an electron of the paramagnetic ion core. The spins of the excess electron and the equivalent paramagnetic core electron are coupled antiparallel, as is illustrated in diagram (5). A set of appropriate, Hund's rule obeying basis functions for the description of the

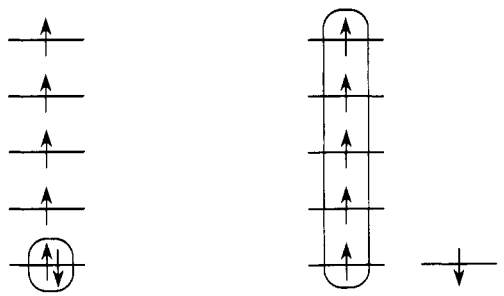

(5) (6)

double-exchange problem in the diiron unit is given by

$$|S_{AB};a\rangle = |[S'_A,(s',s)s'_p = 0]S_A, (s'', S'_B)S^0_B, S_{AB};aab\rangle \quad (10a)$$

$$|S_{AB};b\rangle = |(S'_A, s')S^0_A, [(s, s'')s''_p = 0, S'_B]S_B, S_{AB};abb\rangle \quad (10b)$$

with $S_A = S'_A = S_B = S'_B = S^0 - {}^1/_2 = 2$, $S^0_A = S^0_B = S^0 = {}^5/_2$, and $s = s' = s'' = {}^1/_2$. S'_A (and S'_B) is the coupled spin of the unpaired, spin-parallel electrons in the four orbitals at the top of the diagram. The orbitals (a or b) indicated in eq 10 are occupied by the electrons carrying the spins s', s, and s'', respectively. The parentheses in the expressions eq 10 define, as before, the order of the spin coupling.

Let us consider the action of the transfer operator on $|S_{AB};a\rangle$. This operator can act on either of the electrons in orbital a and yields

$$t_{AB}|S_{AB};a\rangle = 2|[S'_A, (s', s)s'_p = 0]S_A, (s'', S'_B)S^0_B, S_{AB};abb\rangle \quad (11)$$

One of the electrons in orbital a is transferred to orbital b; however, its spin remains coupled to spin s' of the electron still occupying orbital a. The transfer-matrix element to site B follows from spin projection of function eq 11 onto the basis state $|S_{AB};b\rangle$. The projection can be performed by a 3-fold spin-recoupling procedure. Firstly, the spin s of the transferred electron is recoupled to the total core spin S^0_A of ion A, as illustrated in diagram (6). The recoupling yields the factor

$$\langle S'_A, (s', s)s'_p = 0, S_A|(S'_A, s')S^0_A, s, S_A\rangle = \sqrt{\frac{2S^0 + 1}{4S^0}} \quad (12)$$

which is readily obtained by application of the standard formula due to Racah.[29] Secondly, the spin s is recoupled to S^0_B, leading to the well-known matrix element for double exchange

$$\langle (S^0_A, s)S_A, S^0_B, S_{AB}|S^0_A,(s, S^0_B)S_B, S_{AB}\rangle = -\frac{S_{AB} + {}^1/_2}{2S^0 + 1} \quad (13)$$

The matrix elements for $n \geq 5$ and for $n < 5$ are of opposite sign due to the reversal of the excess-electron spin relative to the core spin. Thirdly, the spin s is locally recoupled to the spin s'' of the paramagnetic core electron occupying orbital b, leading to a projection factor equal to that obtained in the first step

$$\langle s,(s'', S'_B)S^0_B,S_B|(s,s'')s''_p = 0, S'_B, S_B\rangle = \sqrt{\frac{2S^0 + 1}{4S^0}} \quad (14)$$

We note that the recoupling procedure entails also a number of terms which do not obey Hund's rule or which are zero due to the Pauli principle, so that they vanish in the projection. By taking the product of equivalence factor 2 (eq 11), of the three recoupling factors, and of β, we arrive at the transfer-matrix element

$$\langle S_{AB};b|t_{AB}|S_{AB};a\rangle = -\beta\frac{S_{AB} + {}^1/_2}{2S^0} \quad (15)$$

Diagonalization of the transfer operator leads to the eigenfunctions

$$\Phi'^{S_{AB}}_{\pm} = \frac{1}{\sqrt{2}}[|S_{AB};a\rangle \mp |S_{AB};b\rangle] \quad (16)$$

with energies

$$E^{S_{AB}}_{\pm} = \pm\beta\frac{S_{AB} + {}^1/_2}{2S^0} \quad (17)$$

where the subscripts $\pm$ correspond to those in $\Phi'^{S_{AB}}_{\pm}$.

The calculation of the transfer-matrix elements thus involves for $n \geq 5$ three recouplings of the excess-electron spin. The local recouplings, however, can be avoided by formally representing the genuine local functions, such as given in diagram (5), by their recoupled versions, such as given in diagram (6). Adopting the same representation in the definition of the basis functions of the dimer yields accordingly

$$|S_{AB};a\rangle \leftrightarrow |(S^0_A, s)S_A, S^0_B, S_{AB};a'\rangle \quad (18a)$$

$$|S_{AB};b\rangle \leftrightarrow |S^0_A, (s, S^0_B)S_B, S_{AB};b'\rangle \quad (18b)$$

The electron of spin s, that will be transferred, is considered to occupy the fictitious orbital a' or b'. The transfer operator is only acting on the electron occupying the primed orbitals in this formulation of the electron-transfer problem. The transfer-matrix elements between basis states eqs 18a and 18b can now be calculated by performing only one single spin recoupling, provided we multiply afterwards all energies by the appropriate correction factor, $(2S^0 + 1)/2S^0$, for equivalence and local recoupling, in order to obtain the matrix elements between the genuine basis functions. The correction factor is equal to ${}^6/_5$ in the system Fe(III)Fe(II). The eigenfunctions correspond in this "intermediate" representation to the expressions

$$\Phi^{S_{AB}}_{\pm} = \frac{1}{\sqrt{2}}[|(S^0_A, s)S_A, S^0_B, S_{AB};a'\rangle \mp |S^0_A, (s, S^0_B)S_B, S_{AB};b'\rangle] \quad (19)$$

where we have dropped the prime of Φ to indicate the difference with the true states. Then, by adopting, as in expression eq 9, a coupling scheme in which the composite core spin, S^0_{AB}, is coupled to the excess-electron spin, s, eq 19 takes the form

$$\Phi^{S_{AB}}_{\pm} = \left[\frac{2S^0 + S_{AB} + {}^3/_2}{2(2S^0 + 1)}\right]^{1/2}|(S^0_A, S^0_B)S^0_{AB} = S_{AB} + {}^1/_2, s, S_{AB};\phi_{\pm}\rangle + \left[\frac{2S^0 - S_{AB} + {}^1/_2}{2(2S^0 + 1)}\right]^{1/2}|(S^0_A, S^0_B)S^0_{AB} = S_{AB} - {}^1/_2, s, S_{AB};\phi_{\mp}\rangle \quad (20)$$

in which the fictitious orbitals $\phi_{\pm}$ are defined by

$$\phi_{\pm} = \frac{1}{\sqrt{2}}(a' \pm b') \quad (21)$$

The functions eq 20 for the system Fe(II)Fe(III) are explicitly given in Table II.

Double Exchange and Vibronic Coupling in Equilateral d^1-d^1-d^2 Systems

Double Exchange. The essential electron-distribution and spin properties of trinuclear mixed-valence clusters linked to double exchange can already be studied in the simplest model system

(29) Brink, D. M.; Satchler, G. R. *Angular Momentum*; Oxford Library of Physical Sciences: Clarendon, Oxford, 1968.

Table II. Energies and Wavefunctions for the d^5-d^6 Double-Exchange Problem

energy	wavefunction constructed on the basis of the intermediate functions (20)
$+\beta$	$\Phi_+^{9/2} = \sqrt{\frac{11}{12}}\lvert S_{AB}^0 = 5, S_{AB} = \frac{9}{2}; \phi_+\rangle + \sqrt{\frac{1}{12}}\lvert S_{AB}^0 = 4, S_{AB} = \frac{9}{2}; \phi_-\rangle$
$+\frac{4}{5}\beta$	$\Phi_+^{7/2} = \sqrt{\frac{5}{6}}\lvert S_{AB}^0 = 4, S_{AB} = \frac{7}{2}; \phi_+\rangle + \sqrt{\frac{1}{6}}\lvert S_{AB}^0 = 3, S_{AB} = \frac{7}{2}; \phi_-\rangle$
$+\frac{3}{5}\beta$	$\Phi_+^{5/2} = \sqrt{\frac{3}{4}}\lvert S_{AB}^0 = 3, S_{AB} = \frac{5}{2}; \phi_+\rangle + \sqrt{\frac{1}{4}}\lvert S_{AB}^0 = 2, S_{AB} = \frac{5}{2}; \phi_-\rangle$
$+\frac{2}{5}\beta$	$\Phi_+^{3/2} = \sqrt{\frac{2}{3}}\lvert S_{AB}^0 = 2, S_{AB} = \frac{3}{2}; \phi_+\rangle + \sqrt{\frac{1}{3}}\lvert S_{AB}^0 = 1, S_{AB} = \frac{3}{2}; \phi_-\rangle$
$+\frac{1}{5}\beta$	$\Phi_+^{1/2} = \sqrt{\frac{7}{12}}\lvert S_{AB}^0 = 1, S_{AB} = \frac{1}{2}; \phi_+\rangle + \sqrt{\frac{5}{12}}\lvert S_{AB}^0 = 0, S_{AB} = \frac{1}{2}; \phi_-\rangle$
$-\frac{1}{5}\beta$	$\Phi_-^{1/2} = \sqrt{\frac{7}{12}}\lvert S_{AB}^0 = 1, S_{AB} = \frac{1}{2}; \phi_-\rangle + \sqrt{\frac{5}{12}}\lvert S_{AB}^0 = 0, S_{AB} = \frac{1}{2}; \phi_+\rangle$
$-\frac{2}{5}\beta$	$\Phi_-^{3/2} = \sqrt{\frac{2}{3}}\lvert S_{AB}^0 = 2, S_{AB} = \frac{3}{2}; \phi_-\rangle + \sqrt{\frac{1}{3}}\lvert S_{AB}^0 = 1, S_{AB} = \frac{3}{2}; \phi_+\rangle$
$-\frac{3}{5}\beta$	$\Phi_-^{5/2} = \sqrt{\frac{3}{4}}\lvert S_{AB}^0 = 3, S_{AB} = \frac{5}{2}; \phi_-\rangle + \sqrt{\frac{1}{4}}\lvert S_{AB}^0 = 2, S_{AB} = \frac{5}{2}; \phi_+\rangle$
$-\frac{4}{5}\beta$	$\Phi_-^{7/2} = \sqrt{\frac{5}{6}}\lvert S_{AB}^0 = 4, S_{AB} = \frac{7}{2}; \phi_-\rangle + \sqrt{\frac{1}{6}}\lvert S_{AB}^0 = 3, S_{AB} = \frac{7}{2}; \phi_+\rangle$
$-\beta$	$\Phi_-^{9/2} = \sqrt{\frac{11}{12}}\lvert S_{AB}^0 = 5, S_{AB} = \frac{9}{2}; \phi_-\rangle + \sqrt{\frac{1}{12}}\lvert S_{AB}^0 = 4, S_{AB} = \frac{9}{2}; \phi_+\rangle$

with electronic configuration d^1-d^1-d^2. The Hamiltonian eq 4 is generalized to polynuclear mixed-valence clusters as follows,[21,22]

$$H_t = \sum_{i<j} \beta_{ij} P_0 t_{ij} P_0 \qquad (22)$$

where the summations run over the magnetic centers, A, B, and C, of the cluster.

In the equilateral symmetry adopted here, the local orbitals a, b, and c, between which the extra electron migrates, are supposed to transform into each other through rotation C_3. The three β_{ij} parameters are equal to a single value, β. The molecular orbital of a symmetry is given by $\phi_a = (a + b + c)/\sqrt{3}$ and has delocalization energy 2β. The orbitals of e symmetry are given by $\phi_{e,1} = (a - b)/\sqrt{2}$ and $\phi_{e,2} = (2c - a - b)/\sqrt{6}$ and have energy $-\beta$. The energy order of the a and e levels defines the sign of β without ambiguity: if the energy of orbital ϕ_a is larger than the energy of ϕ_e, the value of β is positive and negative for the reversed order. The following scheme shows two sets of localized orbitals possessing positive (diagram (7)) and negative (diagram (8)) overlap charge densities, implying, respectively, negative and positive values for the electron-transfer parameter β.

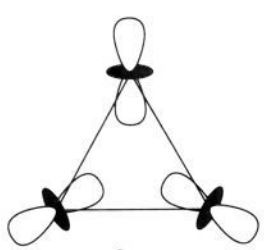

$\beta < 0$

(7)

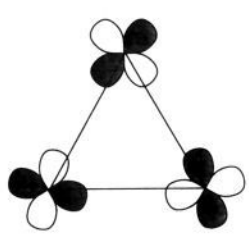

$\beta > 0$

(8)

We adopt, as for the dimer, a basis of electronic states which obey Hund's rule. As we are dealing with a four-spin problem, including three core spins S_i^0, i = A, B, C, and excess-electron spin s, there exists a considerable freedom in the choice of the order of spin coupling in the definition of the electronic basis states. In our numerical analyses of trinuclear systems use is made of the localized basis

Table III. Energies and Eigenstates for the Equilateral d^1-d^1-d^2 Double-Exchange Problem

energies	levels labeled in C_3 symmetry	energies	levels labeled in C_3 symmetry
2β	^{5}A	0	^{3}A
$+\frac{3}{2}\beta$	^{3}E	$-\beta$	^{5}E, ^{3}A, ^{3}E, ^{1}A
$+\frac{1}{2}\beta$	^{1}E		

$$\lvert (S_i^0, S_j^0) S_{ij}^0, (S_k^0, s) S_k, S; k\rangle \qquad (23)$$

The site occupied by the excess electron is noted at the end of the ket. The spins in eq 23 are coupled in three stages. Firstly, the spin s of the excess electron, occupying orbital k, is coupled with core spin S_k^0 to resultant local spin S_k, taking into account Hund's rule. Secondly, the core spins S_i^0 and S_j^0 of the remaining two sites are coupled to give subspin S_{ij}^0. Thirdly, the local spin S_k and spin S_{ij}^0 are coupled to resultant total spin S.

In the application to the system d^1-d^1-d^2, the core spins, S_i^0, i = A, B, C, are equal to $^1/_2$, and the spin of the site containing the excess electron is equal to 1, due to Hund's rule. The subspin S_{ij}^0 of the coupled pair (i,j) is equal to 0 or 1, and the total spin S is 0, 1, or 2. The dimensions of the subspaces for spins S = 2 and 0 are equal to 3, since the excess electron can occupy three sites and the subspin is restricted to one value, $S_{ij}^0 = 1$. For S = 1, the basis has dimension 6, since the spin S_{ij}^0 can now take the values 0 and 1.

The Hamiltonian matrices of the transfer operator eq 22 are obtained by straightforward calculation.[30] Diagonalization yields the electronic energy eigenvalues given in Table III. The labels refer to symmetry group C_3. The energy spectra for spins S = 2 and S = 0 consist of a single A and a single E term, as found in the monoelectronic trimer. The energies for S = 2 are equal to those of the one-electron system, since the delocalization of the excess electron is not affected by the parallel alignment of the core spins. For S = 0 the resonance splitting is reduced by a factor of $-^1/_2$ as a consequence of the antialignment of the core spins. For spin S = 1 there is a mixing of states with

(30) Belinskii, M. I. *Mol. Phys.* **1987**, *60*, 793–819.

different S_{ij}^0 values, leading to a more extended interaction matrix. We note that the energy level at $-\beta$ is highly degenerate, and, as will be shown below, this feature is of crucial importance for the phenomenon of electron delocalization over a pair.

Vibronic Coupling. The relaxation of ligand shell upon addition of the excess electron in a localized state is accounted for by adding the electron-vibrational interaction term eq 24 to the Hamiltonian

$$\mathcal{H}_{ev} = \sum_i \lambda Q_i n_i \tag{24}$$

where λ is the vibronic coupling parameter independent of spin S, Q_i is the totally symmetric local distortion around center i, and n_i is the occupation operator of center i. In the study of the cluster, we pass for convenience to symmetrized coordinates, which for an equilateral triangle read

$$Q_a = \frac{1}{\sqrt{3}}(Q_A + Q_B + Q_C)$$

$$Q_\theta = \frac{1}{\sqrt{6}}(2Q_C - Q_A - Q_B)$$

$$Q_\epsilon = \frac{1}{\sqrt{2}}(Q_A - Q_B) \tag{25}$$

and transform according to the representations a and e of the symmetry group C_{3v}. $\mathcal{H}_{ev}$ can be rewritten as

$$\mathcal{H}_{ev} = \lambda\left[\frac{1}{\sqrt{3}}Q_a + \frac{1}{\sqrt{6}}Q_\theta(2n_C - n_A - n_B) + \frac{1}{\sqrt{2}}Q_\epsilon(n_A - n_B)\right] = \lambda\left[\frac{1}{\sqrt{3}}Q_a + Q_\theta n_\theta + Q_\epsilon n_\epsilon\right] \tag{26}$$

The interaction with vibration Q_a is identical for all electronic states and can therefore be ignored. The diagonalization of the total Hamiltonian matrix yields the electronic energies as a function of the coordinates Q_θ and Q_ϵ. In order to calculate the potential surface, the elastic energy of the nuclear vibrations $^1/_2\sum_{i=A,B,C}\kappa Q_i^2$, where κ is the force constant of the metal-ligand bond which is assumed to be independent of the oxidation state, must be added. Transformation (25) allows us to write the elastic energy in Q_ϵ space as

$$E_{el} = \frac{\kappa}{2}(Q_\theta^2 + Q_\epsilon^2) \tag{27}$$

The vibrations are treated in semiclassical approximation, so that vibrational wavefunctions and vibrational kinetic energies are not examined here.

Pair-Localization in d^1-d^1-d^2. The total Hamiltonian matrix for spin $S = 2$ is equal to that of the monoelectronic system d^0-d^0-d^1 which leads, for equal parameter values, to identical adiabatic surfaces.[31-33] A same formal analogy exists for spin $S = 0$ if we substitute $-\beta/2$ for β in the Hamiltonian matrix of the monoelectronic system. The results for the monoelectronic system follow from the interaction of the three electronic states (one A and two E) with doubly degenerate vibrations of e-symmetry. They have been described several times in the literature[31-33] and are summarized in Figures 1 and 2. The figures display the section along Q_θ axis because one of the minima of the potential surfaces is positioned in this direction for all values of the ratio $\beta/(\lambda^2/2\kappa)$. The surfaces possess third-order symmetry, and two similar sections can be found by the rotations over $\pm 2\pi/3$ in (Q_θ, Q_ϵ) space. For $\beta < 0$ with $|\beta/(\lambda^2/2\kappa)|$ increasing, there is a

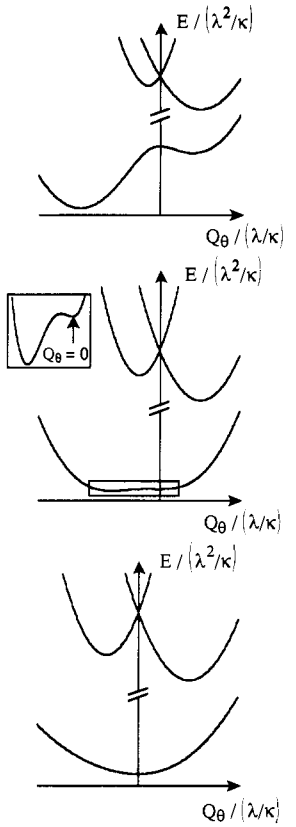

Figure 1. Sections of adiabatic potential surfaces for a monoelectronic mixed-valence trinuclear system along the coordinate Q_θ, obtained for $\beta < 0$ at small, intermediate, and large value of ratio $\beta/(\lambda^2/2\kappa)$. The inset in 1b displays the bottom of the lowest adiabatic potential surface at a smaller energy scale.

transformation from a surface with three minima with three saddle points between them (Figure 1a) to a surface with one minimum (Figure 1c), through an intermediate adiabatic potential with four minima (Figure 1b). The minimum at negative $Q_\theta/(\lambda/\kappa)$ as well as the two equivalent minima describe a nuclear configuration in which the coordination shell of one metal ion is dilated and the two other shells are contracted, leading to preferential localization of the excess electron at one metal site. Thus, the surfaces given in Figure 1 describe excess-electron localization on one site (Figure 1a), delocalization over three centers ($Q_\theta = Q_\epsilon = 0$) (Figure 1c), and coexistence of localized and delocalized electronic distributions (Figure 1b). In the case of positive β, the ground state of E symmetry is affected by the Jahn–Teller effect with the e-vibrations and by the pseudo-Jahn–Teller mixing with the A-state (Figure 2). For $\beta/(\lambda^2/2\kappa) \to \infty$, when the latter interaction may be neglected, the adiabatic surface of the ground state has the well-known shape of a Mexican hat[34] (Figure 2c). The delocalization in this case is not, as for $\beta < 0$, associated with a fixed minimum of C_{3v} symmetry at the origin ($Q_\theta = Q_\epsilon = 0$), but it has a dynamic character due to the presence of a continuum of minima with the same energy. For finite values of $\beta/(\lambda^2/2\kappa)$ the Mexican-hat shaped potential is distorted and three minima appear with localized electronic distributions (Figure 2, parts a and b). In summary, we can say that for spin $S = 0$ and $S = 2$ the excess electron is either localized at one site or delocalized over the whole cluster. The saddle points between the localized minima correspond to electron delocalization over pairs.

The problem of the adiabatic calculation for the $S = 1$ state is qualitatively different from the previous cases, due to its higher dimensionality. In particular, the absolute minimum does not

(31) Launay, J.-P.; Babonneau, F. *Chem. Phys.* **1982**, *67*, 295–300.
(32) Borshch, S. A.; Kotov, I. N.; Bersuker, I. B. *Chem. Phys. Lett.* **1982**, *89*, 381–384.
(33) Cannon, R. D.; Montri, L.; Brown, D. B.; Marshall, K. M.; Elliott, M. C. *J. Am. Chem. Soc.* **1984**, *106*, 2591–2594.
(34) Bersuker, I. B. *The Jahn–Teller Effect and Vibronic Interactions in Modern Chemistry*; Plenum: New York, 1984.

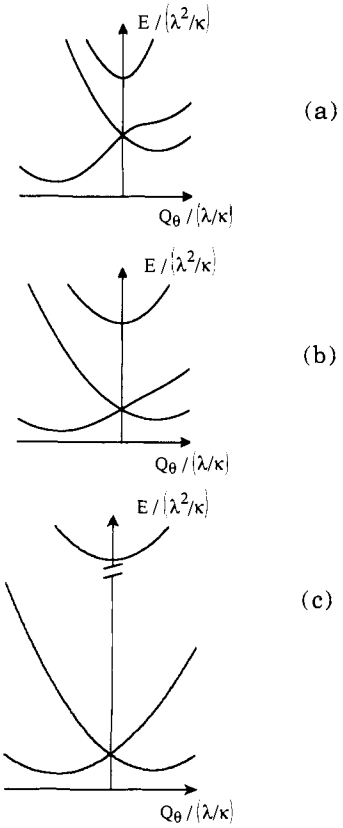

Figure 2. Sections of adiabatic potential surfaces for a monoelectronic mixed-valence trinuclear system along the coordinate Q_θ, obtained for $\beta > 0$ at small, intermediate, and large value of ratio $\beta/(\lambda^2/2\kappa)$.

always lie on the Q_θ axis. For small positive values of the ratio $\beta/(\lambda^2/2\kappa)$ ($0 \le \beta/(\lambda^2/2\kappa) \le 1.42$), one has three minima and three saddle points along the same directions as for the other spin states (Figure 3a). The minima correspond to the same electronic distribution as before, i.e., excess-electron localization at one site. For increasing $\beta/(\lambda^2/2\kappa)$ ($1.42 \le \beta/(\lambda^2/2\kappa) \le 1.50$), two new minima appear instead of each minimum (Figure 3b). At further increase of the $\beta/(\lambda^2/2\kappa)$ value ($1.50 \le \beta/(\lambda^2/2\kappa)$), the minima convert pairwise to the directions of the saddle points obtained for small $\beta/(\lambda^2/2\kappa)$ values (Figure 3c). In other words, we arrive at electron distributions in which the excess electron is homogeneously distributed over *two* sites of the trinuclear cluster in the limit of large $\beta/(\lambda^2/2\kappa)$ values. This delocalization pattern is inherent to the degenerate combination of the ^{3}A and the ^{3}E eigenstates of the transfer operator. This phenomenon is analogous to that established in the theoretical study of the $S = 2$ state in the Fe(II)Fe(III)Fe(III) system, taking into account the same basic interactions, i.e., double exchange and vibronic coupling.[25] Hence, one deals with a quite general property of delocalized magnetic mixed-valence systems.

For negative β values, the ground state of the triplet manifold is an isolated ^{3}E level, which gives rise to a Mexican-hat shaped potential surface in the limit $|\beta/(\lambda^2/2\kappa)| \to \infty$.

Analysis of the Pair-Localization Phenomenon. The numerical analysis in the previous section revealed the possibility of vibronic electron trapping in a pair. In order to gain a deeper insight into this phenomenon, the electronic states will be analyzed using an electronic basis adapted to the broken C_s symmetry. We consider distortions Q_θ, leading to the distinction of the center C at the symmetry plane and the centers A and B at equivalent positions off the plane.

The electronic basis is constructed by spin coupling of the fragments AB and C of the cluster

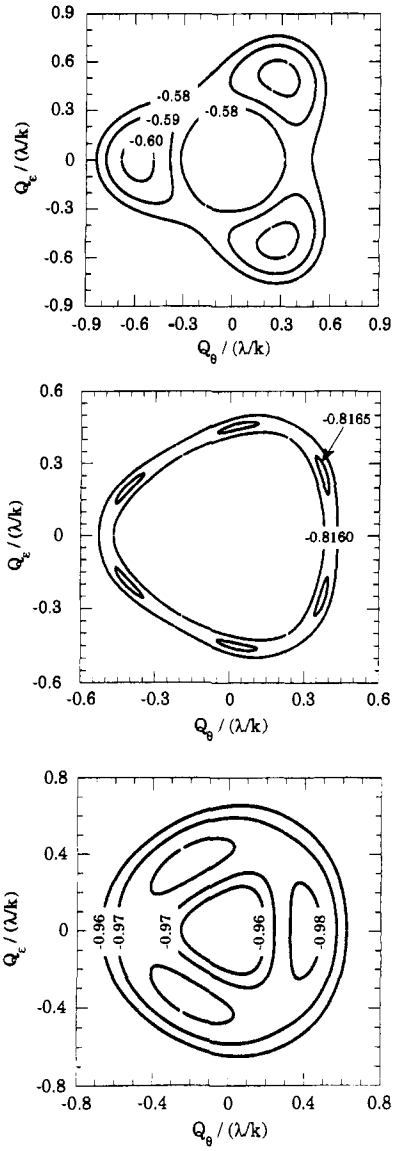

Figure 3. Equipotential curves on lowest adiabatic surface for spin $S = 1$ in the system d^1-d^1-d^2, calculated for positive β at different values of ratio $\beta/(\lambda^2/2\kappa)$: (a) 1.000, (b) 1.466, (c) 1.800. The energy values indicated on the equipotential curves are in units of λ^2/κ. In (a), the excess electron is localized on one site, in (b), it starts to delocalize and in (c), it is delocalized in a pair.

$$|S_{AB}, S_C^0, S\rangle^{\pm} = |\Phi_{\pm}^{S_{AB}}, S_C^0, S\rangle = -\left[\frac{2S^0 - S_{AB} + {}^1/_2}{2(2S^0+1)}\right]^{1/2} \times |(S_{AB}^0 = S_{AB} + {}^1/_2, s)S_{AB}, S_C^0, S;\phi_{\mp}\rangle + \left[\frac{2S^0 + S_{AB} + {}^3/_2}{2(2S^0+1)}\right]^{1/2} |(S_{AB}^0 = S_{AB} - {}^1/_2, s)S_{AB}, S_C^0, S;\phi_{\pm}\rangle \quad (28a)$$

$$|S_{AB}^0, S_C, S;c\rangle = |(S_A^0, S_B^0)S_{AB}^0, (S_C^0, s)S_C, S;c\rangle \quad (28b)$$

The wavefunctions of the fragment AB in eqs 28a and b describe the pair, respectively, in presence and in absence of the excess electron. Correspondingly, the wavefunction of the third center, C, represents an ion in oxidized and reduced state. The total spin can take the values $|S_{AB} - S_C^0| \le S \le |S_{AB} + S_C^0|$ in eq 28a and $|S_{AB}^0 - S_C| \le S \le |S_{AB}^0 + S_C|$ in eq 28b. The expression at the right-hand side of eq 28a is obtained by substitution of expression eq 9 and shows the appearance of the molecular orbitals $\phi_{\pm}$ of the pair.

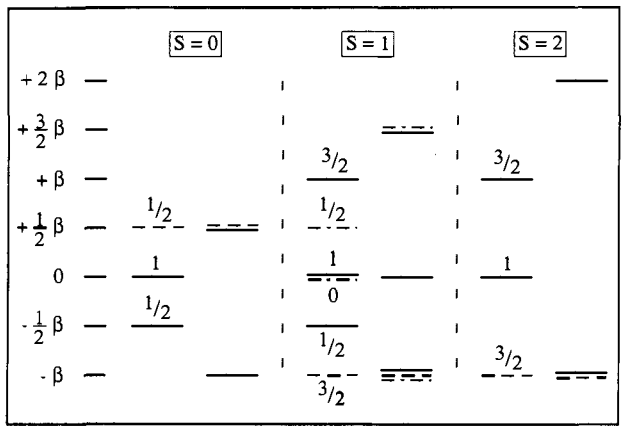

Figure 4. Construction of the double-exchange levels for a d^1-d^1-d^2 equilateral triangle by the pair + site method. For each value of total spin S, energies of the C_{3v} eigenstates (right) and of the C_s symmetry adapted basis (left) are shown. Lines of the same style mean that the states mix to give the eigenstates. The numbers indicate subspin S_{AB} of C_s symmetry adapted basis states. S_{AB} is half integer when AB is the mixed-valence d^1-d^2 pair and is integer when AB is the d^1-d^1 pair.

The delocalization energies of the basis states with the electron occupying the pair AB (eq 28a) depend on spin S_{AB} and are given by the level scheme eq 6 for double exchange, while the energies of the localized basis states (eq 28b) are zero (see Figure 4).

The eigenfunctions of the electron-transfer operator (eq 22) can be expressed in terms of the basis functions given in eq 28 by diagonalizing the Hamiltonian matrices constructed in that basis. The interaction matrix for the operator of electron transfer within the pair (t_{AB}) is diagonal in this basis. The only nondiagonal interactions left involve the operator of electron transfer toward center C ($t_{AC} + t_{BC}$), which connects the states in eq 28a with the states in eq 28b. The evaluation of the interactions is facilitated by two selection rules. The first rule follows from the action of the transfer operator $t_{AC} + t_{BC}$ on the molecular orbitals in the pair AB

$$(t_{AC} + t_{BC})|\phi_+\rangle = \frac{1}{\sqrt{2}}(|c\rangle + |c\rangle) = \sqrt{2}|c\rangle \qquad (29a)$$

$$(t_{AC} + t_{BC})|\phi_-\rangle = \frac{1}{\sqrt{2}}(|c\rangle - |c\rangle) = 0 \qquad (29b)$$

In other words, *electron transfer from orbital ϕ_- to c is forbidden (first selection rule)*. Hence, application of the transfer operator $t_{AC} + t_{BC}$ on the basis functions in eq 28a annihilates the ϕ_- configuration. The ϕ_+ configuration is transformed by the transfer operator into a state, which is a linear combination of basis state eq 28b and a state violating Hund's rule. The spin projection factor on basis state eq 28b can be calculated by recoupling of the excess-electron spin s: from $(S^0_{AB}, s)\,S_{AB}$ to $(S^0_C, s)\,S_C$, using Racah's theorem. The recoupling procedure entails that the value of the subspin S^0_{AB} in the original state (eq 28a) and in the transferred state (eq 28b) does not change: $\Delta S^0_{AB} = 0$ (*second selection rule*). The selection rules imply that a site-localized state (eq 28b) cannot interact with more than two pair-delocalized states (eq 28a), so that the electronic eigenstates are linear combinations of at most one site-localized and two pair-delocalized states.

The basis states and the resulting C_s symmetry-adapted eigenstates are indicated in Figure 4 in the example d^1-d^1-d^2. The basis states interact as follows: (1) In the spin $S = 2$ space: basis state $|S_{AB} = {}^3/_2, S^0_C = {}^1/_2, S = 2\rangle^-$ does not interact with any other basis state. The basis state $|S_{AB} = {}^3/_2, S^0_C = {}^1/_2, S = 2\rangle^+$ interacts with $|S^0_{AB} = 1, S_C = 1, S = 2; c\rangle$. (2) In the spin $S = 1$ space: basis state $|S_{AB} = {}^3/_2, S^0_C = {}^1/_2, S = 1\rangle^-$ does not interact with any other basis state. The basis states $|S_{AB} = {}^1/_2, S^0_C = {}^1/_2, S = 1\rangle^-$ and $|S_{AB} = {}^3/_2, S^0_C = {}^1/_2, S = 1\rangle^+$ contain the components $|S^0_{AB} = 1, S_{AB} = {}^1/_2, S = 1; \phi_+\rangle$ and $|S^0_{AB} = 1, S_{AB} = {}^3/_2, S = 1; \phi_+\rangle$, respectively, and thus interact with $|S^0_{AB} = 1, S_C = 1, S = 1; c\rangle$. The basis state $|S_{AB} = {}^1/_2, S^0_C = {}^1/_2, S = 1\rangle^+$ contains the configuration $|S^0_{AB} = 0, S_{AB} = {}^1/_2, S = 1; \phi_+\rangle$ and interacts with basis state $|S^0_{AB} = 0, S_C = 1, S = 1; c\rangle$. (3) In the $S = 0$ subspace: the basis state $|S_{AB} = {}^1/_2, S^0_C = {}^1/_2, S = 0\rangle^-$ contains the configuration $|S^0_{AB} = 1, S_{AB} = {}^1/_2, S = 0; \phi_+\rangle$ and interacts with basis state $|S^0_{AB} = 1, S_C = 1, S = 0; c\rangle$. The basis state $|S_{AB} = {}^1/_2, S^0_C = {}^1/_2, S = 0\rangle^+$ contains the component $|S^0_{AB} = 0, S_{AB} = {}^1/_2, S = 0; \phi_+\rangle$ but does not interact with $|S^0_{AB} = 1, S_C = 1, S = 0; c\rangle$ since the value of the subspin S^0_{AB} in the component is different from that in the basis state. The resulting energy spectrum coincides, evidently, with that of Table III but now the composition of the electronic eigenstates is adapted to C_s symmetry.

The analysis of the effect of distortion Q_θ on the electronic states is considerably facilitated by the introduction of the C_s symmetry-adapted basis, since operator $\lambda Q_\theta n_\theta$ is diagonal in this basis. The only effect of the distortion is to shift the energies of the pair-localized basis functions given in eq 28a relative to the energies of the site-localized states in eq 28b. These shifts change the relative weights of the basis functions in the composition of the electronic eigenstates. However, in the limit of strong transfer interaction, $|\beta/(\lambda^2/2\kappa)| \to \infty$, the vibronic modulation of the electronic eigenstates becomes vanishingly small, so that the C_s symmetry-adapted eigenstates for $Q_\theta = 0$ are approached. In other words, the off-diagonal elements of $\lambda Q_\theta n_\theta$ in the set of C_s symmetry-adapted eigenfunctions can be ignored in this limit. The structural relaxations along the coordinate Q_θ, induced by the inhomogeneous electron distributions in these eigenfunctions, are proportional to the values of the vibronic matrix element $\langle 2n_C - n_A - n_B\rangle$. The vibronic stabilization energy is given by the expression

$$E_{vib} = \langle 2n_C - n_A - n_B\rangle^2 \frac{\lambda^2}{12\kappa} = \langle 3n_C - 1\rangle^2 \frac{\lambda^2}{12\kappa} \qquad (30)$$

The last expression in eq 30 follows from the former by taking into account the normalization condition $n_A + n_B + n_C = 1$. The vibronic stabilization energy is thus a function of the occupation of center C.

Values for occupation number n_C and stabilization energy E_{vib}, calculated for the C_s symmetry-adapted ground states of the system d^1-d^1-d^2 obtained for $\beta > 0$ are presented in Table IV. The ground states can be described as follows (see Figure 4): (1) For spin $S = 2$, an eigenstate equal to the basis state $|S_{AB} = {}^3/_2, S^0_C = {}^1/_2, S = 2\rangle^-$, in which the excess electron is exclusively delocalized within pair AB ($\langle n_C\rangle = 0$) of maximum spin, which is coupled parallel to S^0_C; a state in which the electron is delocalized over the three centers, with major contribution at site C ($\langle n_C\rangle = {}^2/_3$; the subspin S_{AB} has no definite value). The two states correspond to the absolute minima described above, i.e.,

Table IV. Average Occupation of Site C ($\langle n_C\rangle$), Vibronic Coupling Parameter ($\langle 3n_C - 1\rangle$), and Vibronic Stabilization Coefficient ($\langle 3n_c - 1\rangle^2$) for the d^1-d^1-d^2 Equilateral Triangle

C_3 labels	C_s adapted basis	$\langle n_C\rangle$	$\langle 3n_C - 1\rangle$	$\langle 3n_C - 1\rangle^2$
^1A		$\frac{1}{3}$	0	0
^3A, ^3E	state 1	0	−1	1
	state 2	$\frac{2}{5}$	$\frac{1}{5}$	$\frac{1}{25}$
	state 3	$\frac{3}{5}$	$\frac{4}{5}$	$\frac{16}{25}$
^5E	state 1	0	−1	1
	state 2	$\frac{2}{3}$	1	1

the minima of the two-branched section of the Mexican hat along the axis Q_θ. (2) For spin $S = 1$, an eigenstate equal to the basis state $|S_{AB} = {}^3/_2, S_C^0 = {}^1/_2, S = 1\rangle^-$, in which the excess electron is exclusively delocalized within the pair AB ($\langle n_C\rangle = 0$) of maximum spin, which is coupled antiparallel to spin S_C^0 (The state is depicted in diagram (9) and corresponds with the pair-delocalized, broken-symmetry state found in the numerical analysis of the previous section.); two states with the excess electron occupying preferentially site C ($\langle n_C\rangle = {}^3/_5$ or ${}^2/_5$), possessing a more complex spin composition. (3) For spin $S = 0$, a state in which the excess electron is homogeneously distributed over the three centers of the system ($\langle n_C\rangle = {}^1/_3$; the subspin S_{AB} has no definite values). Maximum vibronic stabilization energies of equal size are obtained for the two spin quintets and the spin-triplet state $|S_{AB} = {}^3/_2, S_C^0 = {}^1/_2, S = 1\rangle^-$.

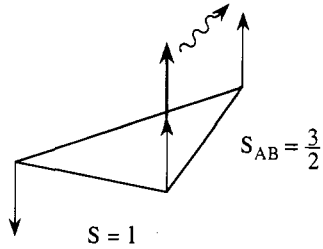

(9)

The analysis of the system d^1-d^1-d^2 can be summarized as follows. For small values of the ratio of electron transfer and vibronic coupling parameters, $|\beta/(\lambda^2/2\kappa)| \ll 1$, the excess electron is vibronically trapped at a single site of the trimer. At larger values of $|\beta/(\lambda^2/2\kappa)|$, numerical calculation reveals in the ground states of spin $S = 1$ and of $S = 2$ structures that are also Jahn–Teller distorted from ideal geometry, even so if the ratio approaches infinity. This property is due to the presence of an orbitally-degenerate electronic ground state for these spin values. The vibronic interactions within the degenerate ground manifold of spin $S = 1$ give rise to breaking of C_{3v} symmetry into C_s symmetry. This kind of symmetry breaking is found when the ground manifold comprises states of different symmetry (A + E) with respect to C_{3v} symmetry. The electronic ground state at the broken-symmetry structure is obtained by antiparallel spin coupling of the pair-delocalized ground state of the dimer ($\Phi_-^{3/2}$) to the core state ($S_C^0 = {}^1/_2$) of the third center: $|S_{AB} = {}^3/_2, S_C^0 = {}^1/_2, S = 1\rangle^-$. For $S = 2$, where we are dealing with a vibronic e^*E problem, the broken-symmetry structures are degenerate and describe a circle around the origin of the (Q_θ, Q_ϵ) plane. The electronic ground state at the intersection with the Q_θ axis ($|S_{AB} = {}^3/_2, S_C^0 = {}^1/_2, S = 2\rangle^-$) has the same spin-coupling scheme as the state for $S = 1$.

The vibronic stabilization of the states $|S_{AB} = {}^3/_2, S_C^0 = {}^1/_2, S\rangle^-$ for $S = 1$ and 2 has the following grounds. Firstly, the selection rules prevent admixture with other states through interaction with distortion Q_θ. Secondly, the optimal C_s structures for these states are, for $\beta/(\lambda^2/2\kappa)$ sufficiently large, stable (or metastable, as in case e^*E) with respect to distortion Q_ϵ. The system with electronic structure $|S_{AB} = {}^3/_2, S_C^0 = {}^1/_2, S = 1\rangle^-$ is thus confined to axis Q_θ. Its structure is stabilized by expansions of the ligand shells accommodating the excess electron. The vibronic stabilization energies for spin $S = 1$ and $S = 2$ are equal. The eigenstate of the form $|S_{AB} = {}^3/_2, S_C^0 = {}^1/_2, S\rangle^-$ is excluded for spin $S = 0$, as it would violate the spin-composition rule, $S \geq |S_{AB} - S_C|$. The eigenstate of spin $S = 0$ is a linear combination of configurations in which the excess electron is occupying the dimeric subunit as well as the remaining center of the trinuclear system, leading to a more homogeneous electron distribution. As a consequence, the structure is in ground state of spin $S = 0$ more stable with respect to distortions from C_{3v} symmetry than in states of higher spin. The vibronic coupling has thus the effect to stabilize the states of spin $S = 1$ and $S = 2$ relative to the state of spin $S = 0$.

The degeneracy of the broken-symmetry ground states of spin $S = 1$ and $S = 2$ can be removed by introducing Heisenberg–Dirac–Van–Vleck exchange. A nondegenerate ground state of intermediate spin ($S = 1$) is found in case of antiferromagnetic exchange, provided that this interaction is moderate; this in order to prevent the stabilization of a spin $S = 0$ ground state.

The excess electron in the ground state of spin $S = 1$ can be trapped in any pair of the trimer. Once trapped, the electron will remain in the same pair, provided that quantum tunneling and thermal activation are negligible. The former effect is normally considerably reduced by small imperfections ("random strains") always existing in real systems. At temperatures T with kT of the same order of magnitude as the heights of the potential barriers separating the minima, the excess electron starts to migrate between the three pair-localized states. The observation of pair localization is then delimited by the spectroscopic time window, which should not exceed the reciprocal of the jumping frequency of the itinerant electron.

Electron Distribution and Spin State in $[Fe_3S_4]^0$

X-ray analyses of trinuclear iron–sulfur proteins and synthetic models, only available for homovalent species, reveal structures of nearly 3-fold (C_{3v}) symmetry for the unit $[Fe(III)_3S_4]^{1+}$ (diagram (10)). In spite of the equivalence of the iron ions in

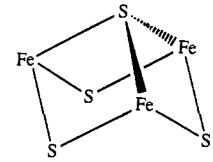

(10)

these clusters, Mössbauer investigations of the reduced species show an accumulation of excess-electron charge at only two centers in the $S = 2$ ground state, indicating a breaking of the initial C_{3v} symmetry into C_s symmetry, similar to that derived in the previous section.

As for the system d^1-d^1-d^2, we performed first a numerical analysis of the adiabatic potential surfaces of the system d^5-d^5-d^6 in (Q_θ, Q_ϵ) space. For ratios $|\beta/(\lambda^2/2\kappa)| \ll 1$, the excess electron is, as expected, vibronically trapped at a single site of the trimer. For increasing values of the ratio, the adiabatic potential surfaces display transformations, depending on spin, similar to those obtained for the system d^1-d^1-d^2 (see, e.g., Figure 3). The analysis shows that for $|\beta/(\lambda^2/2\kappa)|$ sufficiently large, one of the broken-symmetry minima in each set of equivalent minima is positioned on the Q_θ axis for all values of the spin S. Therefore, we adopt, in the construction of the electronic states, again a C_s symmetry-adapted basis, which is constructed by spin coupling of the molecular fragments AB and C:

$$|S_{AB}, S_C^0, S\rangle^{\pm} = |\Phi_{\pm}^{S_{AB}}, S_C^0, S\rangle \leftrightarrow \left[\frac{2S^0 + S_{AB} + \frac{3}{2}}{2(2S^0+1)}\right]^{1/2} \times \left|\left(S_{AB}^0 = S_{AB} + \frac{1}{2}, s\right) S_{AB}, S_C^0, S; \phi_{\pm}\right\rangle + \left[\frac{2S^0 - S_{AB} + \frac{1}{2}}{2(2S^0+1)}\right]^{1/2} \times \left|\left(S_{AB}^0 = S_{AB} - \frac{1}{2}, s\right) S_{AB}, S_C^0, S; \phi_{\mp}\right\rangle \quad (31a)$$

$$|S_{AB}^0, S_C, S; c\rangle \leftrightarrow |(S_A^0, S_B^0) S_{AB}^0, (S_C^0, s) S_C, S; c'\rangle \quad (31b)$$

The basis states eqs 31a and 31b describe the system with pair-

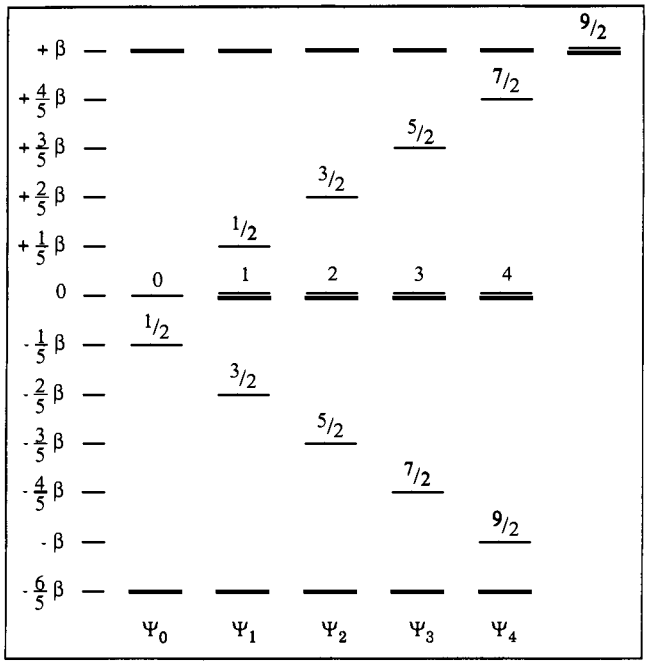

Figure 5. Construction of the double-exchange levels for the $S = 2$ subspace of a d^5-d^5-d^6 equilateral triangle by the pair + site method. C_s symmetry adapted basis states (normal face), fulfilling selection rules (see text), are arranged in columns, together with resulting C_{3v} eigenstates (bold face). The numbers indicate subspin S_{AB} of C_s symmetry adapted basis states. S_{AB} is half integer when AB is the mixed-valence d^5-d^6 pair and is integer when AB is the d^5-d^5 pair. The Ψ_4 state is the one experimentally observed in $[Fe_3S_4]^0$ (see text).

delocalization over AB and site-localization at C, respectively, and are illustrated in the diagrams (11) and (12). The expression at the right-hand side of eq 31a is obtained, after passing to intermediate representation, by substitution of eq 20. The values

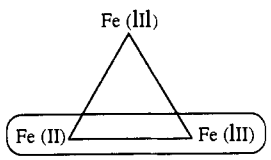

(11)

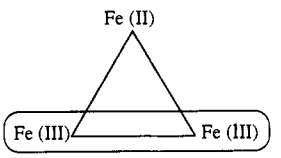

(12)

for the triplets (S_{AB}, S^0_C, S) in eq 31a and of (S^0_{AB}, S_C, S) in eq 31b, fulfilling the spin-composition rules $|S_{AB} - S^0_C| \le S \le |S_{AB} + S^0_C|$ and $|S^0_{AB} - S_C| \le S \le |S^0_{AB} + S_C|$, respectively, are listed in Table V.

The process of formation of C_s symmetry-adapted eigenstates is represented in Figure 5 in the example of spin $S = 2$. The energies of the basis states in eq 31a are equal to the pair-delocalization energies, given in eq 17. One can construct two pair-delocalized basis states of total spin $S = 2$, with energies of opposite signs, for each value of S_{AB}. There is one site-localized state (eq 31b) of spin $S = 2$ for S^0_{AB} equal to 0, 1, 2, 3, and 4. The state of total spin $S = 2$ and subspin $S^0_{AB} = 5$ is excluded, since $S < |S^0_{AB} - S_C|$. The energies of the states in eq 31b are zero.

The selection rules, stated above, imply that the Hamiltonian matrices constructed in basis eq 31 can be decomposed into submatrices of dimensions less than or equal to three. The diagonalizations of the Hamiltonian matrices can be performed analytically and yield the energy eigenvalues indicated in Figure 5. The electronic ground state of spin $S = 2$ is 5-fold degenerate for positive β values. The C_s symmetry-adapted eigenfunctions, Ψ_i, $i = 0$–4, are linear combinations of the basis states given in the same column of Figure 5. For example, the eigenfunction Ψ_4 is given by the expression

Table V. Spin Values for the Triangle Fe(III)–Fe(III)–Fe(II) in the Pair + Site Approach

$S^{(0)}_{AB}$ Fe(III)–Fe(III)	$S^{(0)}_C$ Fe(II)	S
0		2
1		1, 2, 3
2	2	0, 1, 2, 3, 4
3		1, 2, 3, 4, 5
4		2, 3, 4, 5, 6
5		3, 4, 5, 6, 7
Fe(III)–Fe(II) or Fe(II)–Fe(III)	**Fe(III)**	
1/2		2, 3
3/2		1, 2, 3, 4
5/2	5/2	0, 1, 2, 3, 4, 5
7/2		1, 2, 3, 4, 5, 6
9/2		2, 3, 4, 5, 6, 7

$$\Psi_4 = \sqrt{\frac{250}{297}}|S_{AB} = \tfrac{9}{2}, S^0_C = \tfrac{5}{2}, S = 2\rangle^- - \sqrt{\frac{2}{297}}|S_{AB} = \tfrac{7}{2}, S^0_C = \tfrac{5}{2}, S = 2\rangle^+ + \sqrt{\frac{45}{297}}|S^0_{AB} = 4, S_C = 2, S = 2;c\rangle \quad (32)$$

The first two terms in eq 32 do not interact, whereas they both do with the third one. The basis state with maximum pair-delocalization energy, $|S_{AB} = {}^9/_2, S^0_C = {}^5/_2, S = 2\rangle^-$, contains a small ϕ_+ component (see eq 31a, second term), through which it can interact with the site-localized state $|S^0_{AB} = 4, S_C = 2, S = 2;c\rangle$. The additional transfer interaction toward center C explains the lowering of the ground state energy, $-6\beta/5$, relative to the pair-delocalization energy, $-\beta$. The energy eigenvalues for spin $S = 2$ and the other spin states are tabulated in Table VI.

For negative values of β, the electron-transfer interaction stabilizes a ground state of spin $S = 7$, which is separated by an energy gap of $-\beta/5$ from the first excited state.

For positive values of β, the ground level, $E = -6\beta/5$, is a highly degenerate manifold, including states of spin ranging from $S = 0$–6. The lowest energy state of spin $S = 7$ has the same delocalization energy, $-\beta$, as a monoelectronic system, and is lying above the ground state energy.

As argued in the previous section, the vibronic stabilization energy at the Q_θ axis of the C_s symmetry-adapted eigenfunctions is a function of the occupation number of center C, which is given in eq 30. The argument $\langle n_C\rangle - {}^1/_3$ in the energy expression measures the deviation from homogeneous electron distribution, i.e., from $\langle n_C\rangle = {}^1/_3$. The vibronic coupling thus selects as ground state the C_s symmetry-adapted function of the ground manifold which possesses the most inhomogeneous excess-electron distribution, i.e., the state for which $|\langle n_C - {}^1/_3\rangle|$ is maximal. The vibronic constants and stabilization energies in the ground manifold are given in Table VII. The table shows that the ground states of spin $S = 0$ and $S = 6$ are orbitally nondegenerate (A state with $\langle n_C\rangle = {}^1/_3$), so that these states are not affected by vibronic interaction. The ground manifolds of spin $S = 1, 2, 3$, 4, and 5, however, are degenerate ($\langle n_C\rangle \neq {}^1/_3$), and they are thus stabilized relative to the $S = 0$ and $S = 6$ states by vibronic interaction. The vibronic couplings in the ground manifolds of spin $S = 2, 3, 4$, and 5 take maximum size in the C_s symmetry-adapted eigenfunctions containing the component $|S_{AB} = {}^9/_2, S^0_C = {}^5/_2, S\rangle^-$, such as the function Ψ_4 given in eq 32. The electron delocalization over the pair AB furnishes the main

Table VI. Energies and Eigenstates for the Equilateral d^5-d^5-d^6 Double-Exchange Problem

energies	levels labeled in C_3 symmetry
$+2\beta$	^{15}A
$+\frac{9}{5}\beta$	^{13}E
$+\frac{8}{5}\beta$	^{11}A, ^{11}E
$+\frac{7}{5}\beta$	^{9}A, ^{9}A, ^{9}E
$+\frac{6}{5}\beta$	^{7}A, ^{7}E, ^{7}E
β	^{5}A, ^{5}A, ^{5}E, ^{5}E
$+\frac{4}{5}\beta$	^{3}A, ^{3}A, ^{3}E
$+\frac{3}{5}\beta$	^{1}E
$+\frac{1}{5}\beta$	^{3}E
0	^{5}A, ^{5}A, ^{5}E
$-\frac{1}{5}\beta$	^{7}A, ^{7}A, ^{7}E, ^{7}E
$-\frac{2}{5}\beta$	^{9}A, ^{9}E, ^{9}E
$-\frac{3}{5}\beta$	^{11}A, ^{11}A, ^{11}E
$-\frac{4}{5}\beta$	^{13}A, ^{13}E
$-\beta$	^{15}E
$-\frac{6}{5}\beta$	^{1}A, ^{3}A, ^{3}E, ^{5}A, ^{5}E, ^{5}E, ^{7}A, ^{7}A, ^{7}E, ^{9}A, ^{9}E, ^{11}E, ^{13}A

contribution to the electronic energy in these states. The eigenstates of spin $S = 1$, however, involving only basis states $|S_{AB}, S_C^0 = {}^5/_2, S = 1\rangle^-$ of smaller subspin, $S_{AB} < {}^9/_2$, possess lower pair-delocalization energies. Hence, the $S = 1$ states require more delocalization toward C in order to attain the ground state energy, and they are therefore less stabilized by vibronic coupling than the states of spin $S \geq 2$. The choice between $S = 2$, 3, 4, and 5 is a more delicate matter, which can be settled, however, by straightforward calculation. The results for the stabilization energies, given in Table VII, show that the largest vibronic energy is found for spin $S = 2$. The electronic wavefunction of the broken-symmetry ground state, Ψ_4, is given by eq 32. The main component of the ground state is $|S_{AB} = {}^9/_2, S_C^0 = {}^5/_2, S = 2\rangle^-$, of which a pictorial represention is given in the following diagram.

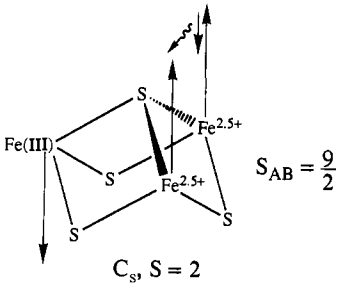

C_s, S = 2

(13)

We remark that this component has been identified by Mössbauer spectroscopic studies of these clusters. The component forms, however, only a part of the exact wavefunction. In view of the smallness of the other two components, it remains questionable whether any detailed information about them can be extracted from Mössbauer investigations.

We note that, although the discussion above is only strictly valid in the limit of large intercenter resonance, a pair delocalized ground state of spin $S = 2$ is already obtained for ratios $\beta/(\lambda^2/2\kappa) \geq 1$.

Table VII. Average Occupation of Site C ($\langle n_C \rangle$), Vibronic Coupling Parameter ($\langle 3n_C - 1 \rangle$), Vibronic Stabilization Coefficient ($\langle 3n_C - 1 \rangle^2$) for the d^5-d^5-d^6 Equilateral Triangle

C_3 labels	C_s adapted basis	$\langle n_C \rangle$	$\langle 3n_C - 1 \rangle$	$\langle 3n_C - 1 \rangle^2$
^{1}A		0.333	0	0
^{3}A, ^{3}E	state 1	0.257	$-\frac{8}{35}$	0.052
	state 2	0.343	$\frac{1}{35}$	0.001
	state 3	0.400	$\frac{1}{5}$	0.040
^{5}A, ^{5}E, ^{5}E	Ψ_4	0.152	$-\frac{6}{11}$	0.298
	Ψ_3	0.273	$-\frac{2}{11}$	0.033
	Ψ_2	0.364	$\frac{1}{11}$	0.008
	Ψ_1	0.424	$\frac{3}{11}$	0.074
	Ψ_0	0.455	$\frac{4}{11}$	0.132
^{7}A, ^{7}A, ^{7}E	state 1	0.167	$-\frac{1}{2}$	0.250
	state 2	0.300	$-\frac{1}{10}$	0.010
	state 3	0.400	$\frac{1}{5}$	0.040
	state 4	0.467	$\frac{2}{5}$	0.160
^{9}A, ^{9}E	state 1	0.192	$-\frac{11}{26}$	0.179
	state 2	0.346	$\frac{1}{26}$	0.001
	state 3	0.462	$\frac{5}{13}$	0.148
^{11}E	state 1	0.238	$-\frac{2}{7}$	0.082
	state 2	0.429	$\frac{2}{7}$	0.082
^{13}A		0.333	0	0

Magnetic Hyperfine Parameters. The magnetic hyperfine Hamiltonian of homovalent systems is easily adapted to mixed-valent systems:[21]

$$\mathcal{H}_{hf} = \sum_i \{\boldsymbol{S}_i[\mathbf{a}_{II}]_i \boldsymbol{I}_i n_i + \boldsymbol{S}_i[\mathbf{a}_{III}]_i \boldsymbol{I}_i (1 - n_i)\} \qquad (33)$$

in case of fractional occupation, $0 < n_i < 1$. The summation in eq 33 is running over the three centers, i = A, B, C, $\boldsymbol{S}_i$ and $\mathbf{I}_i$ are the electron-spin and nuclear-momentum operators of center i, respectively, and $[\mathbf{a}_{II}]_i$ and $[\mathbf{a}_{III}]_i$ are the magnetic hyperfine coupling tensors of the iron ion at site i in the oxidation states indicated. We pass in eq 33 from local spin $\boldsymbol{S}_i$ to total spin $\boldsymbol{S}$, using the Wigner–Eckart theorem

$$\mathcal{H}_{hf} = \sum_i \boldsymbol{S}[\mathbf{A}]_i \mathbf{I}_i \qquad (34)$$

The effective coupling tensors $[\mathbf{A}]_i$ can be expressed in terms of the local coupling parameters (taking $[\mathbf{a}] = a[\mathbf{1}]$) by equating

$$A_i\langle \boldsymbol{S} \rangle = a_{II}\langle \boldsymbol{S}_i n_i \rangle + a_{III}\langle \boldsymbol{S}_i (1 - n_i) \rangle \qquad (i = \text{A, B, C}) \quad (35)$$

in which $\langle\,\rangle$ is indicating the expectation value in the electronic state considered. A straightforward calculation yields for the ground state Ψ_4 the expressions

$$A_A = A_B = \frac{38\,669}{112\,266} a_{II} + \frac{11\,371}{20\,412} a_{III}$$

$$A_C = -\frac{10}{99} a_{II} - \frac{139}{198} a_{III} \qquad (36)$$

Table VIII. Component-Averaged Magnetic Hyperfine Parameters in Proteins and Models

center	A^{av}_{AB}, MHz	A^{av}_{C}, MHz	ref
Fe_3S_4 in *D. gigas* FdII	-19.1	+15.6	12
Fe_3S_4 in aconitase	-17.8[a]	+16.8	*b*
$[Fe_3S_4(LS_1)Fe(t\text{-}BuNC)_3]^{1-}$	-16.2	+14.3	15
$[Fe_3S_4(SEt)_3Mo(CO)_3]^{1-}$	-16.9	+15.2	16
$[Fe_3S_4(SBz)_3Mo(CO)_3]^{3-}$	-18.1[a]	+15.3	16
calculated[c]	-18.8	+16.3	this work

[a] Mean of values at sites A and B. [b] Surerus, K. K.; Kennedy, M. C.; Beinert, H.; Münck, E. *Proc. Natl. Acad. Sci. U.S.A.* 1989, *86*, 9846. [c] Obtained using $a_{II} = -22.2$ and $a_{III} = -20.0$ MHz (see text).

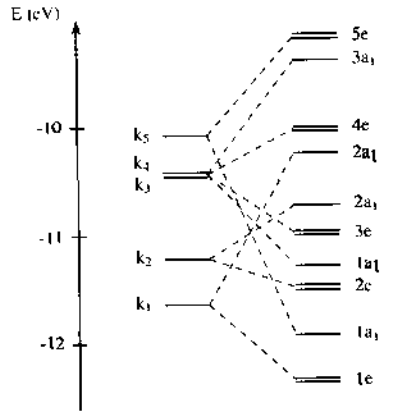

Figure 6. Energies of the 15 highest d-rich orbitals for the $[Fe_3S_4]^0$ core (right). Energies of the deduced 15 Wannier orbitals (left), k_{1-5} ($k = a, b, c$). Note that the k_{1-1} come from the *e* set of T_d symmetry and that k_{3-5}, from the t_1 set. The excess electron moves in the k_1 set which forms the 1e and $2a_2$ molecular orbitals with $2a_1$ above 1e.

The A_i values at centers A and B are equal, but different from that at site C, due to symmetry breaking. The choice of empirical coupling constants a_{II} and a_{III} was discussed in ref 12 and the averaged parameters $a_{II} = -22.2$ and $a_{III} = -20.0$ MHz were proposed. Substitution of these values into eq 36 gives $A_A = A_B = -18.8$ MHz and $A_C = +16.3$ MHz, which are close to the values -19.1 and +15.6 MHz, respectively, found in reduced FdII.[11] We note that the model considering excess-electron delocalization strictly confined to a pair gives hyperfine parameter values, $A_A = A_B = -19.2$ and $A_C = +16.7$ MHz, also in a good agreement with the experimental data for FdII. We would like to stress, however, that the *A* values from ref 12 follow from an *ad hoc*, postulated electronic structure, whereas they result in the present study from a theoretical model which takes into account the basic interactions in the system. The theoretical and experimental results for FdII and of related compounds are summarized in Table VIII.

Values of Model Parameters. The fundamental parameters of our model are the electron-transfer interaction, β, and the vibronic stabilization energy $\lambda^2/2\kappa$. Their values can, in principle, be estimated from analysis of experimental data or by theoretical calculation. Since empirical data for β are not available, we have to resort to theoretical estimates of this parameter. In order to verify that $\beta > 0$ and to get an estimate of its value, we performed an extended Hückel calculation on the Fe_3S_4 cluster using the crystal structure data of the 3Fe(III) system but with an idealized C_{3v} symmetry.[35] The thiolate groups were approximated by S^{2-} anions. The 15 highest d-rich molecular orbitals are represented in Figure 6. They can be transformed into a set of Wannier orbitals by

$$a = \frac{1}{\sqrt{3}}\phi_a - \frac{1}{\sqrt{6}}\phi_\theta + \frac{1}{\sqrt{2}}\phi_t$$

(35) Girerd, J.-J., unpublished results.

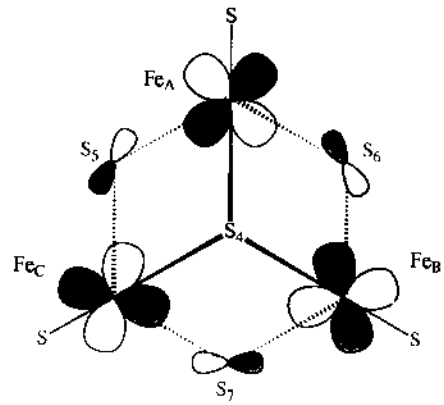

Figure 7. Schematic drawing of the strongly antibonding molecular orbital $2a_2$.

$$b = \frac{1}{\sqrt{3}}\phi_a - \frac{1}{\sqrt{6}}\phi_\theta - \frac{1}{\sqrt{2}}\phi_\epsilon$$

$$c = \frac{1}{\sqrt{3}}\phi_a + \frac{2}{\sqrt{6}}\phi_\theta \qquad (37)$$

i.e., a set of equivalent orthogonal orbitals, centered at the sites A, B, and C, respectively. The energies of the Wannier orbitals are represented on the left-hand side of the figure. We obtain, for instance at center *A*, five orbitals a_{1-5} which are distributed as expected for a distorted local T_d geometry: an "*e*" set including a_{1-2} and a "t_2" including a_{3-4-5}. The a_1 orbital is a $d_{x^2-y^2}$ like orbital pointing approximately along the bisecting lines of S_4-Fe_AS_5 and $S_4Fe_AS_6$ angles. The a_2 orbital is a d_{z^2} like orbital pointing approximately along the bisecting line of the S_4Fe_AS angle. The extra electron migrates between the orbitals a_1, b_1, and c_1. The main result for our purpose is that these orbitals give an a_2 molecular orbital at energy -10.24 eV and an *e* set at -12.34 eV. This shows that $\beta = +0.7$ eV. The sign of β can be qualitatively understood from Figure 7 which represent schematically the molecular orbital $2a_2$: it is clearly antibonding. In view of the approximate nature of the method we do not attach great value to the exact number calculated for β: only its sign and order of magnitude are of significance. The positive sign confirms the preceding analysis. The trinuclear iron–sulfur systems were also studied by Noodleman et al., using the broken-symmetry, density-functional method.[36] However, the energy levels thus obtained do not match the spectrum of the double-exchange Hamiltonian, and require the introduction of spin-dependent β values, which may differ by a factor of ten. The origin of this discrepancy needs further analysis.

In order to estimate the vibronic stabilization energy from empirical data we adopt the procedure introduced by Schatz et al. in a study of the Creutz-Taube complex.[37] The vibronic constant λ is proportional to the difference in iron-sulfur distances in the two oxidation states. The expression for the shift in the totally symmetric local coordinate reads

$$\Delta Q = \frac{\lambda}{\kappa} \qquad (38)$$

From the definition of normal coordinate for a tetrahedral complex MX_4 we get

$$\Delta Q = \frac{1}{2}\sum_i \Delta r_i = 2\Delta r \qquad (39)$$

(36) Noodleman, L.; Case, D. A. In ref 5, pp 423–470. Noodleman, L.; Case, D. A.; Sontum, S. *J. Chim. Phys.* 1989, *86*, 743–755. Sontum, S.; Noodleman, L.; Case, D. A. In *The Challenge of d and f Electrons: Theory and Computation*; Salahub, D. R., Zerner, M. C., Eds.; ACS Symposium Series, 1989; Vol. 394, pp 366–377. Note that the parameter *B* used in this reference is connected with our β by $B = \beta/5$.

(37) Wong, K. Y.; Schatz, P. N. *Prog. Inorg. Chem.* 1981, *28*, 369–449.

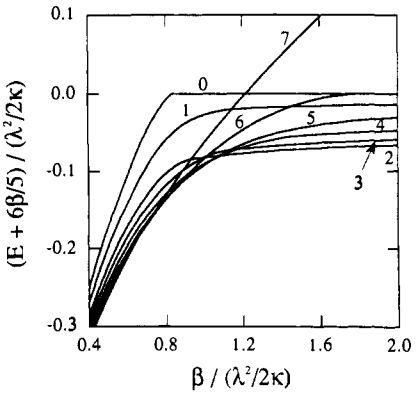

Figure 8. Relative spin-state energies (numbers are indicating spin S), at the absolute minima of the adiabatic potential surfaces as a function of the ratio of the electron-transfer parameter, β, and the vibronic stabilization energy, $\lambda^2/2\kappa$.

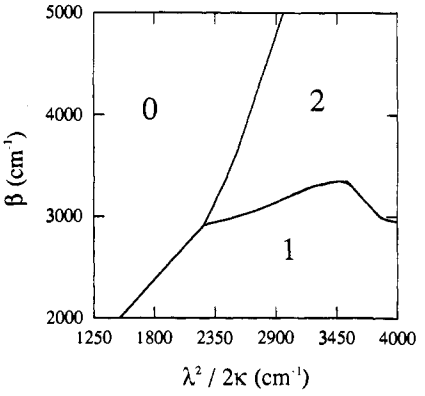

Figure 9. Spin of ground state (S = 0, 1, or 2) in the presence of antiferromagnetic exchange, $J = -160$ and $J_1 = -360$ cm^{-1}, as a function of electron-transfer parameter, β, and vibronic stabilization energy, $\lambda^2/2\kappa$.

Using eqs 38 and 39, and $\kappa = M\omega^2$ (M is the mass of the ligand, and $\omega = 2\pi\nu$ is the angular frequency of vibration) we obtain the following expression for the vibronic energy

$$\frac{\lambda^2}{2\kappa} = 2M\omega^2(\Delta r)^2 \qquad (40)$$

The value of Δr in mononuclear iron–sulfur complexes is found to be of the order of 0.1 Å,[38] and the symmetrical stretching vibrational quanta vary from 250 to 450 cm^{-1}.[39] These data provide us with the range 1200 cm^{-1} $\leq \lambda^2/2\kappa \leq$ 3860 cm^{-1}, for the vibronic stabilization energy. The transfer interactions and vibronic couplings in iron–sulfur systems are thus of the same order of magnitude. It can be seen from Figure 8, that the spin of ground state is S = 2 for values of the ratio $\beta/(\lambda^2/2\kappa)$ appropriate to iron–sulfur clusters. The energy gap between the S = 2 ground state and the lowest excited state of spin S = 3 varies from 10 to 30 cm^{-1} in the range mentioned. This energy gap is rather small but it can be considerably enhanced by antiferromagnetic exchange.

Effect of Antiferromagnetic Exchange. Until now we ignored the antiferromagnetic exchange interaction between the high-spin iron ions in the triiron cluster. Studies of the magnetic properties of polynuclear Fe–S clusters reveal that the exchange interactions in these systems are of considerable magnitude. They can be incorporated in the model by adding the Hamiltonian

$$\mathcal{H}_{ex} = -\sum_{k,i,j}[J\mathbf{S}_k\cdot(\mathbf{S}_i + \mathbf{S}_j) + J_1\mathbf{S}_i\cdot\mathbf{S}_j]n_k \qquad (41)$$

where the summation is running over the labels (k, i, j) = ABC, CAB, and BCA. The Hamiltonian takes into account the different values of the exchange-coupling constants for ferrous–ferric (J) and ferric–ferric interaction (J_1).

The most reliable estimates of the exchange parameters are obtained in dimeric iron–sulfur clusters, which exhibit localized mixed-valence states: $|J| \geq 160$ cm^{-1} for ferrous–ferric interaction and $|J_1| \geq 360$ cm^{-1} for ferric–ferric interaction.[9]

Let us consider first the case of equal exchange parameters, $J = J_1$. Under this condition the spin-state energies are shifted by the amount $-JS(S + 1)/2$. The eigenfunctions, however, remain unchanged. The energy gaps separating the S = 2 ground state from the states with spins $S > 2$ increase by antiferromagnetic exchange, whereas the gaps with the S = 0 and S = 1 states are reduced, and they may even change in sign. Values of $|J|$ larger than 60 cm^{-1} are already sufficient to change the ground-state spin from 2 to 0 for any value of vibronic stabilization energy in the interval mentioned above. The nonequivalence of the exchange parameters, $|J| < |J_1|$, must be taken into account to preserve a spin S = 2 ground state. In order to investigate the effect of antiferromagnetic exchange, we determined the spin of the ground state in the ranges of β and $\lambda^2/2\kappa$ values appropriate to the iron–sulfur clusters, by means of numerical calculation of the adiabatic surfaces for the d^5-d^5-d^6 cluster, adopting J and J_1 values characteristic for these systems.[9] The results, presented in Figure 9, show that the spin of the ground state can be S = 0, 1, or 2. A ground state of spin S = 2 is obtained in the domain of the figure with stronger transfer and vibronic interactions. Analysis of the electron distributions at the minima of the adiabatic potentials shows that the excess electron is mainly delocalized over a pair in the parameter domain with ground state spin S = 2. The ground state of S = 2 has also been interpreted in the framework of a purely electronic HDVV model with $|J| \leq 0.4\,|J_1|$.[40] However, this approach does not explain the electronic distribution observed in iron–sulfur trimers.

Conclusion

The main results of this work can be summarized as follows.

(i) The framework of an effective-Hamiltonian approach to describe the electronic properties of mixed-valent iron–sulfur clusters, taking into account the effects of double exchange, vibronic coupling, and HDVV exchange, is formulated.

(ii) The theory of double exchange in symmetric dinuclear units is reformulated by introducing molecular orbitals, $\phi_\pm$, in the description of the itinerant electron therein. The eigenfunctions of the unit can be interpreted as linear combinations of two configurations in which the electron occupies the orbitals ϕ_+ and ϕ_-. The weights of the two configurations approach 1 and 0 in high-spin states and $^1/_2$ in states of lower spin.

(iii) The electronic ground state of the equilateral mixed-valent system Fe(III)Fe(III)Fe(II) is for $\beta < 0$ an orbitally nondegenerate state of maximum spin. For $\beta > 0$, the electronic ground state is degenerate, including several states of different spin.

(iv) Vibronic coupling in equilateral trimers traps the excess electron at one of the sites in the limit of small electron-transfer interaction, $\beta/(\lambda^2/2\kappa) \to 0$. For larger interactions, the electron starts to delocalize. The delocalization process, however, does not necessarily end up in an equal distribution over the three sites of the unit when we approach the limit $\beta/(\lambda^2/2\kappa) \to \infty$. The condition for partial delocalization, and concomitant symmetry breaking of the structure, is the presence of an orbitally degenerate

(38) Lane, R. W.; Ibers, J. A.; Frankel, R. B.; Papaefthymiou, G. C.; Holm, R. H. *J. Am. Chem. Soc.* **1977**, *99*, 84–98.
(39) Yachandra, V. K.; Hare, J.; Moura, I.; Spiro, T. G. *J. Am. Chem. Soc.* **1983**, *105*, 6455–6461.
(40) Bertini, I.; Briganti, F.; Luchinat, C. *Inorg. Chim. Acta* **1990**, *175*, 9–10.
(41) Borshch, S. A.; Bominaar, E. L.; Girerd, J.-J. *New J. Chem.* **1993**, *17*, 39–92.

ground state. Vibronic coupling in ground manifolds including electronic states of different symmetry (transforming according to irreducible representations A and E in C_{3v} symmetry) leads to stabilization of pair-delocalized states. This phenomenon is found in the system Fe(III)Fe(III)Fe(II), for spin S = 1, 2, 3, and 4 (see also ref 41).

(v) The degeneracy in the electronic ground manifold of Fe(III)Fe(III)Fe(II), obtained for $\beta > 0$, is removed by vibronic coupling. The coupling results in a broken-symmetry ground state of spin S = 2, in which the electron is mainly delocalized over two sites of the trimer. The energy gap separating the S = 2 ground state from the next S = 3 state is only a small fraction of the vibronic site-localization energy, $\lambda^2/2\kappa$. The gap is, however, considerably enhanced by antiferromagnetic exchange.

(vi) The spin, the charge distribution, and the magnetic hyperfine parameters calculated in the electronic ground state of Fe(III)Fe(III)Fe(II) are in good agreement with the experimental data for these quantities.

(vii) The positive sign of β, needed in the interpretation of the data of $[Fe_3S_4]^0$ clusters, is confirmed by extended Hückel calculation.

(viii) The introduction of antiferromagnetic exchange does not change the main conclusions as obtained without this interaction. For realistic values of the exchange-coupling constants J and J_1 there is a large domain in the $(\beta,\lambda^2/2\kappa)$ space in which a pair-delocalized state of spin S = 2 is ground state.

Applications in several directions will be considered in the future: description of the ground-state properties of mixed-valent $[MFe_nS_m]^k$ clusters with different compositions and oxidation levels and description of excited-state properties, notably the intervalence bands in the S = 2 manifold of the $[Fe_3S_4]^0$ cluster.